



# Load Dependence Behavior of The Thermoelectric Module Energy Harvesting System by Inverse Dynamic Analysis–Maximum Power Point Tracking

R. Mohamed<sup>1\*</sup>, A. M. Yusop<sup>2</sup>, A. Mohamed<sup>1</sup> and N.A. Sulaiman<sup>2</sup>

<sup>1</sup>Centre for Integrated Systems Engineering and Advanced Technologies (Integra), Faculty of Engineering and Built Environment, Universiti Kebangsaan Malaysia, 43600 UKM Bangi, Selangor, Malaysia

<sup>2</sup>Centre for Telecommunication Research and Innovation (CeTRI), Fakulti Kejuruteraan Elektronik dan Kejuruteraan Komputer, Universiti Teknikal Malaysia Melaka, Hang Tuah Jaya, 76100 Durian Tunggal, Melaka, Malaysia

\*Corresponding author E-mail: [ramizi@ukm.edu.my](mailto:ramizi@ukm.edu.my)

## Abstract

This paper presents the characterization behavior of a thermoelectric module (TEM) analysis by the implementation of a new inverse dynamic analysis–maximum power point tracking (IDA-MPPT), with different load resistance values to the common maximum power point circuit (MPPC) controller. In this study, a conventional TEM test unit measurement is performed consists of a hotplate and a TEM module. The two MPPC boards are fed with the harvested voltage from the TEM module and a supercapacitor is linked with it. The load resistor is then fed with the boosted voltage of the second board. The three phases experimental analysis is introduced in a closed loop manner. There are, TEM system analysis without the IDA-MPPT implementation, TEM system analysis with IDA-MPPT implementation, and a newly developed IDA-MPPT unit experimental analysis. Results have shown that the TEM system with IDA-MPPT implementation with 1k $\Omega$  resistor is capable of achieving 5V output stable line voltages with 83.33% efficiency. In conclusion, with the input stable voltage of the MPPC board from the new input –shaping process, a satisfactory load behavior is achievable by its voltage readings.

**Keywords:** closed-loop; inverse dynamic analysis; load dependence; maximum power point tracking, thermoelectric.

## 1. Introduction

Renewable energy has becoming a wide research interest in order to reduce the dependence of the fossil fuel. Fossil fuel is known to expose the world to a hazardous environment in air pollution, hazardous waste emission, depletion of ozone and saturated carbon that harm to lives. Hence scientific development to find alternative energy has becoming more popular for future development. Among common alternative energy devices that currently being employed are photovoltaic system, thermoelectric, and piezoelectric. Among those are, thermoelectric modules (TEM) that have recently being considered as an alternative energy that capable of converting wasted energy into useful one [1-6]. It converts waste heat dissipated energy or ambient heat energy, harvested to the its system into useful electrical power to power up small useful devices. It is known to have no moving parts, which has an advantage of operating at longer period compare to others with no maintenance required [7,8].

Most TEMs are widely known used for cooling mechanisms [9-11], however other alternatives used have been discovered in many applications such as in domestic woodstove [12-14], charger [15,16], automotive system [17] and exhaust gases [18,19]. Other than that, both cooling and heating applications of thermoelectric devices also have been utilized [20-22]. Other researchers examining the characterization of the thermoelectric devices, which extending beyond the usual applications of the modules [23]. For example, Carmo *et al.* [24] has presented a methodology of characterization of the thermoelectric generator modules with an application to different type of loads. The SPICE simulation software has been used to model the developed experiment, in which the researchers has made an arrangement in such away that the internal resistance in a series, whereby the output voltage variation is plotted against various temperature measurements.

Other study also has focus on to the characterization at low temperature [25]. They have performed the thermoelectric characterization of Seebeck coefficient based on electrical conductivity and temperature dependencies at a temperature range of 100<sup>0</sup>K to 375<sup>0</sup>K. Their finding was that the applications are very much suitable under low temperature, in which they have claimed that the 250<sup>0</sup>K is the critical temperature point of their meticulous thermoelectric generator. Collectively, to the Seebeck effect characterization analysis, Under steady state condition, Kossovakis *et al.* [26] had studied and examined the TEM performance. Based on the computational data collected and made in comparison to the available manufacturer's data, they have proved the analysis has a significant improvement in term of energy efficiency.

This paper is presenting an analysis of the thermoelectric behavior of TEM modules as main source of energy harvester. In addition, a new maximum power point tracking (MPPT) circuit is added along with voltage and current measurement. Previous reviews have shown that, the focus was onto the voltage and current output characteristics only. Meanwhile, the effect of the existence of MPPT circuit be-

behavioral analysis has given less significant emphasized has been put on. The new proposed MPPT circuit that has been presented in [27-30], will be discussed in this study, To ensure the reliability of the model, TEPI-12656-0.6 TEMs modules were used to accomplish the stated principal idea.

## 2. Experimental Setup

Fig. 1 shows the experimental arrangement for the characterization of the load dependence behavior of the proposed TEM system. It is purposely to validate the performance of the proposed new method of the suggested MPPT, by using an inverse dynamic analysis-maximum power point tracking (IDA-MPPT), which has been presented in a closed loop manner of our previous studies [27,29,30]. Verification is a necessary in order to prove that the proposed MPPT method will give a good behavioral output with an additional of load resistor to prolong the sustainable stable supply. As shown, the rig unit consists of a 2.5V 5F super capacitor (from Cooper Bussmann), two maximum power point circuit (MPPC) board (DC 1587 from Linear Technology) and a selected load resistance value.

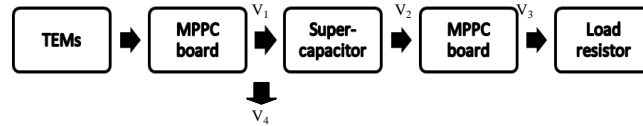


Fig. 1: Block diagram of the TEM system.

Two MPPC boards were used to perform maximum power point tracking on each process. The supercapacitor is used as a temporary storage to feed for the secondary MPPC board before feeding it the load resistor. In other word the load resistor received a boosted voltage of  $V_3$  as a result from two stages MPPCs. The performance of the MPPT process is by considering the output voltage of the proposed TEM system. The consideration is by looking at the output voltage to have a stable output supply of 5V, in which the MPPC board can supply at its maximum rating. Two modes of operations have been identified for the MPPC board: 'ON' and 'OFF' state. Under the 'ON' state, the MPPC board will received energy from the TEM module continuously. Under the 'OFF' state, the MPPC will retain the most recent process of energy received and stop calculating the energy harvested from the TEM. In active condition, the supercapacitor is continuously receive energy (charging) from the MPPC board during the 'ON' state while the system is charging other devices. Thus, the supercapacitor will have a continuous maximum rating charged capacity during this state. The setup shown in Fig. 1, have shown that there are several test point to verify the system performance. This is essential in order to track the behavioral analysis of the proposed TEM system module developed. NI-USB 6211 (Data Acquisition Card from National Instruments) is used to performed all the recorded said test point. It is continuously monitored and displayed in MATLAB environment.

The TEMs used in the analysis are arranged in series electrically and arranged in parallel thermally. In other words, the series connection is to obtain maximum voltage and parallel connection is to dissipate heat effectively across the module [30]. In this way, the arrangement configurations of the TEMs portray the actual design implementation in real applications. In total six TEMs were used from Thermodynamic Module type (TEPI-12656-0.6), for which the detail specifications are listed in Table 1.

The experimental setup consists of hot surface (a hotplate module CB 160 from Stuart) as to provide control hot source energy to the TEM modules. The hot surface was set to a temperature of  $50^{\circ}\text{C}$ , with air natural cooling on the other side. With this arrangement, it provides a transient conditions to the TEM modules without any fixed constant cooling system, such as heat sink, in order to give actual behavior under dynamic transient conditions. If in any case the experiment is conducted with the implementation of a heat sink, the system would be in steady state condition, which needs to be avoided. In order to see the behavioral effect of IDA-MPPT on the load voltage, the analysis has to be conducted in transient conditions. To complete the measurements, a thermocouple is placed on each sides of the TEM modules, and were connected to a data logger. TC-08 PicoLog data logger were used from Pico Technology and directly connected to a computer in real time. The complete test unit is shown in Fig. 2.

Table 1: Specifications of the TEM (TEPI-12656-0.6)

Specifications	Values
Hot side temperature ( $^{\circ}\text{C}$ )	300
Cold side temperature ( $^{\circ}\text{C}$ )	30
Open circuit voltage (V)	8.4
Matched load resistance ( $\Omega$ )	1.2
Matched load output voltage (V)	4.2
Matched load output current (A)	3.4
Matched load output power (W)	14.6
Heat flow across the module (W)	$\approx 365$
Heat flow density ( $\text{W cm}^{-2}$ )	$\approx 11.6$
AC resistance measured at $27^{\circ}\text{C}$ and 1000 Hz ( $\Omega$ )	0.5-0.7

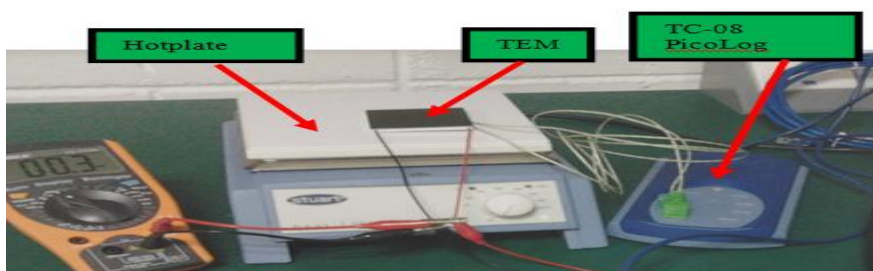


Fig. 2: Detailed experimental setup of the TEM system showing the TEPI-12656-0.6 TEM placed on top of the hotplate. The TC-08 PicoLog data logger is used to record the temperature data measured by the thermocouple.

In the procedure, it starts by setting 'ON' state to both MPPC boards. In this mode, the supercapacitor will continuously receive harvested voltage as recorded by the NI-USB 6211 from the first MPPC board. The rated voltage specified was at 1.8V, from which it was set to jumper JP1, and also closest to supercapacitor rating voltage. The charging process starts as soon as the MPPC board boosted the voltage to its rated value and was capped at that level, similarly to the jumper set point. The second phase of the charging process begins when the second MPPC board starts to receive voltage and begin calculating the sufficient energy required for the supercapacitor to charge another device. The existence of the load at the end of the system will likely to force the output voltage to drop to nearly 0V, however, the presence of the second MPPC board will likely to maintain the output level at its maximum rating. Thus a suitable MPPT scheme is employed in the experiment in order to maintain and reach boosted peak voltage at maximum and to reach the end load voltage at its maximum point. In this way, the analysis of the scheme with and without IDA-MPPT can be achieved and the advantage of the proposed scheme with the load dependence behavior can be clarified.

### 2.1. TEM with IDA-MPPT

The purpose of have the second MPPC board is to maintain the output level at its maximum 5V level without the IDA-MPPT. It is however, the boosted voltage level becomes unstable once the output resistor is loaded. Hence, the effect of IDA-MPPT to the load variation is investigated further, which describe in this subsection. Initially, the purpose of having IDA-MPPT is to reshape the harvested energy from the TEM output based on the actual raw input to the system and replicating the desired output voltage by the MPPC board. Thus Fig. 3 shows the replicating process with an additional input shaper into the IDA-MPPT scheme. The improve scheme, the IDA-MPPT, involves both input shaper and the existing MPPC board. Based on the nature, the term 'input shaper' denotes to the point that shaping the input signal that fed into the developed system. Process detail of the said technique will be elaborated in the following subsection.

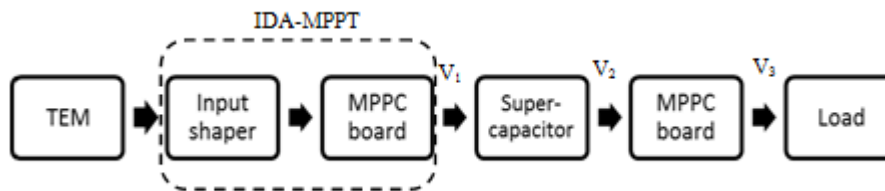


Fig. 3: Block diagram of the TEM system and the input shaper with the new tapped voltage.

### 2.2. Inverse dynamic analysis

The term inverse dynamic analysis (IDA), shows the process of distinguishing the obtainable output response from input function of the system. In doing so, the output response of the system should be determined first, before implementing IDA. The outcome of applying IDA to the system, become explicable once the output response has been identified from the MPPC board output voltage. The first order system of transfer function will be employed in the technique, which starts computing the output response. The controller will portray a feed forward system with no feedback measurement which may allow to degrade the performance of the system, due to its high power consumption of the device measurements. The behaviour of the overall systems starts by computing its transfer function that very much dependence on the following equation:

$$V(u) \times F(u) = X(u) \quad (1)$$

where  $V(u)$  is the normalized TEM or SA voltage function,  $F(u)$  is the normalized input of the TEM, and  $X(u)$  is the normalized desired output function.  $F(u)$  can be derived by substituting the function of the system and the desired output into Eq. (1). In designing the IDA, before deriving the input function, a selection of a suitable output function must be prioritized first. A third order function of the exponential type input function has been resolved to be the best candidate among the existing types of output response as presented from various researchers. The details discussion of the third order selection can be found in [29]. The named exponential third order function is shown as follows:

$$x(t) = X_E [1 - e^{-u^3}] \quad (2)$$

Where the normalized time  $u$  can be defined as follows:

$$u = \alpha t \quad (3)$$

where  $\alpha$  is the generalized term between time and the normalized time. Next is the normalized equation of the desired output function that can be obtained from Eqs. (2) and (3):

$$X(u) = \frac{x(t)}{X_E} = 1 - e^{-u^3} \quad (4)$$

The boosted output voltage out of the MPPC board has shown to be similar to the first derivative of the third-order exponential function in its final result of [29]. Hence, the logical relationship,  $X(u)$  can be derived as follows:

$$X(u) = X(\dot{u}) = 3u^2 e^{-u^3} \quad (5)$$

Equation (5) shows the relationship of the desired output function to its equivalent exponential function. In other word, the first derivative of the third order exponential function and the exponential function behaves similarly. With these derivations, the IDA-MPPT process proceeds by shaping the harvested output voltage of the TEM modules after the desired output voltage has been declared. The shaping process is to ensure that the third order exponential response behavior is being followed by the input response of the first MPPT board. Knowing this there is higher possibility that the output response of the loaded TEM will follow exactly the behavior of the boosted energy of the MPPT board. In this way, the technique exhibits a way to have voltage response stability regardless whether the system is loaded or unloaded.

From the context description of the technique, the input function of IDA-MPPT will be as follows:

$$F(u) = \frac{1 - e^{-u^3}}{V(u)} \times n \quad (6)$$

where  $n$  is the voltage multiplier (the third-order exponential function response has settled to a maximum value that the MPPT should obtain). Towards the end, the behavioral analysis can be performed, in which maintaining system stability and maintaining maximum output voltage with loaded or unloaded resistors.

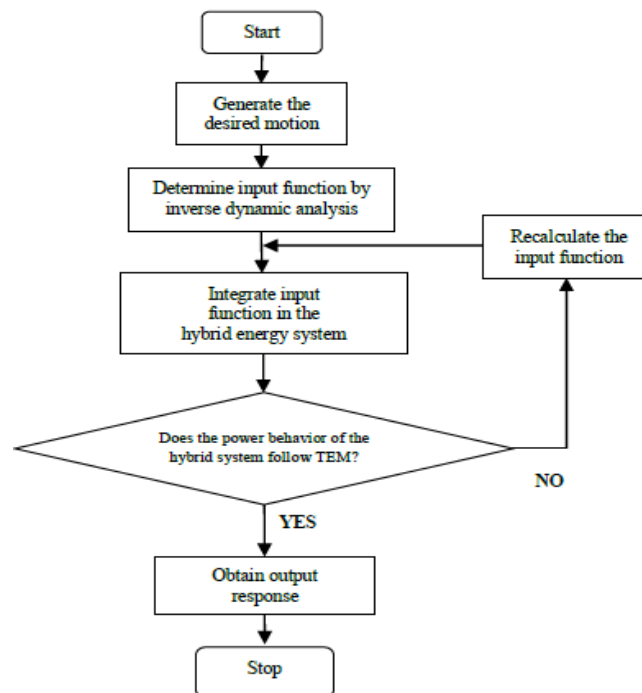


Fig. 4: Design process of the inverse dynamic analysis

Fig. 4 shows the design process of the inverse dynamic analysis technique. First the desired output function needs to be determined. This exponential type input shaper in Eq. 4 is used to indicate the output function. From there, the input function is derived as in Eq. 6. The inverse dynamic analysis of the exponential type of the input shaper technique is used to simulate the input voltage of the energy harvesting system. Then the output power behaviour of energy of the hybrid energy harvesting circuit is compare with the output power behaviour of TEM. If the power behaviour of both systems is same, then the output response of the overall system can be obtained.

### 3. Results and Discussion

The first behavioral analysis results of the TEM load dependence is merely on the analysis of loaded response with different resistance values. The three load resistance ( $R_L$ ) values being considered were, 6.6  $\Omega$ , 13.2  $\Omega$ , and 1 k $\Omega$ . These values were selected based on the typical application of mobile device charger input impedance classified as Type A and Type B. The Type A charger has an input loading resistance of 7 $\Omega$  or 13 $\Omega$ , with voltage 7V and current of 0.7A input requirements. The Type B charger has in input loading resistance of 1k $\Omega$ , with a voltage of 5V and a current of 0.35A.

From these classified input requirements, it is categorized to have that the current of Type B charger is 50% of the Type A charger. Similarly, the input load resistance of the Type B charger is 200% of the Type A charger. A 1k $\Omega$  resistor is selected, in order to emulate for higher end charging devices which may have higher different input loading resistance. Again, the analysis is presented into two parts, before control strategy implementation and after control strategy implementation. And for every analysis, it will give result analysis on the different loaded resistors of 6.6  $\Omega$ , 13.2  $\Omega$ , and 1 k $\Omega$ .

#### 3.1. TEM without IDA-MPPT control strategy

The output results analysis begins with given a full load implementation to the TEM system proposed. In this way, it can determine the effect of loading the system and analyse its behaviour for given different load resistors. As shown in Fig. 5, when the system is loaded with small resistance values, the output response is closed to 0V. However, when 1k $\Omega$  resistor is loaded, a significant difference is clearly seen. Where the system begins to react supplying the energy to other devices. With  $R_L = 6.6 \Omega$  and  $R_L = 13.2 \Omega$ , the system capable of supplying the energy of about 20s only to the load.

When changing the  $R_L$  to  $1k\Omega$ , the energy is supplied for about 40s. The domain of supplying the energy by the TEM is called the time active zone. Figs. 5(a) and 5(b) show that the output loaded voltage almost zero, which shows instability throughout the analysis, even though the MPPC board two produces 5V output. In contrast, when replacing the output load to  $1k\Omega$  resistor, a significant different is clearly seen where the minimum voltage is about 0.1V only.

With  $R_L = 1k\Omega$ , the output of the second MPPC board drop suddenly from 5V to almost zero, as has shown in Fig. 5(c) of Zone 1. However, at the same time the load voltage represented by the diamond marker, increased abruptly from 0 V to 3.4 V with a current of 3.4 mA. Upon attaining this value, the load voltage decreases significantly to 0.1 V for 145 s until the load is disconnected. At this instant the current value measured was around 100  $\mu$ A.

Next, the load resistor is disconnected swiftly, as shown in Fig. 5(c), zone 2. During this time the boosted voltage slightly increases to 1.2V, but yet to reach its maximum level. It is believe due to the voltage of the supercapacitor that does not reach its specified limit to boost the voltage back to 5V level. The voltage stabilizes at 1.2V until the supercapacitor is fully charge at its minimum level. From the reading analysis acquired, it was found out that, once the supercapacitor has reach a voltage of about 0.4394 the output load voltage reaches its maximum level, as has shown in zone 3.

The next experimental analysis will be considered after the second MPPC board failed to stabilize and stay at its maximum level, in which IDA-MPPT will be employed to the loaded TEM. The analysis has been carried out because IDA has proven to shape the TEM output it its desired response. The objective of the behavioral analysis is to maintain the system at 5V level maximum, throughout the whole time of the experiment regardless of the loaded  $R_L$ .

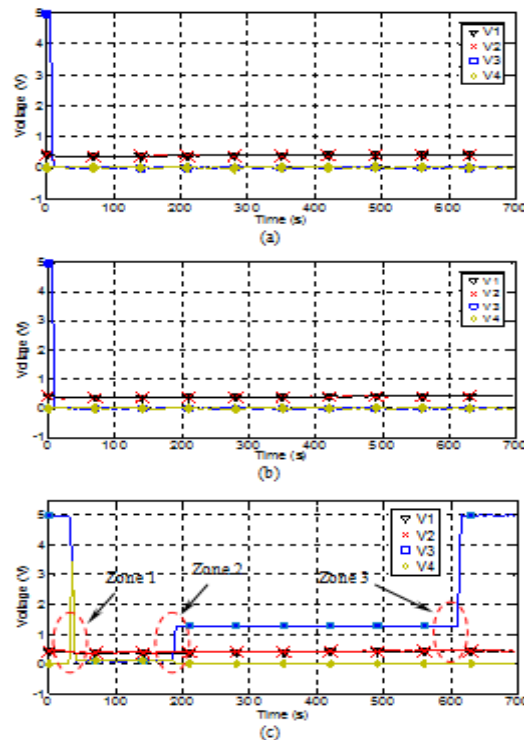


Fig. 5: Voltage profile of the TEM after being loaded with different values of  $R_L$ . (a)  $R_L = 6.6\Omega$ . (b)  $R_L = 13.2\Omega$ . (c)  $R_L = 1k\Omega$ .

### 3.2. TEM with IDA-MPPT control strategy

The proposed IDA-MPPT control strategy was developed to stabilize the proposed system to boost and maintain the voltage level for the MPPC boards at its maximum point at the stipulated time. The purpose of having IDA is to initially shape the harvested energy out of the TEM to meet the system requirement of stable 5V output. Although, analytically the system would be able to shape and maintain its voltage level, the end voltage level would still be very much dependant on the loaded output resistance value that connected to the system. Hence to see the variance of the behavioural analysis the same output loaded resistance will be utilized in order to see the significant used of the IDA technique.

Figs. 6(a) and 6(b) show a similar voltage behaviour at all measurement test points for both  $R_L = 6.6\Omega$  and  $R_L = 13.2\Omega$  respectively. With  $R_L = 6.6\Omega$ , the load voltage has increased to 1.2V by the influence of IDA-MPPT technique. However for  $R_L = 13.2\Omega$ , the load voltage has a significant impact with the IDA-MPPT technique with slightly higher and reach an initial voltage level approximately to 1.8V similar to supercapacitor voltage level. The supercapacitor voltage level under the influence of IDA-MPPT technique has a notable similar value to the boosted voltage level of the first MPPC board. In comparison with the previous system without the IDA-MPPT implementation, the IDA-MPPT implementation has a boosted voltage level of 30s period, rather than at its lowest 0V load voltage. Even yet from this analysis, with the lower output load resistance the voltage level has reacted to the IDA-MPPT technique but the voltage level has not yet reaching 5V.

To verify the results,  $1k\Omega$  resistor is loaded to the system. As shown in Fig. 6(c), the supercapacitor voltage level is stable and maintain at 1.8V, similar to the capped value level set by the MPPC board. In contrast to the two responses of Figs. 6(a) and 6(b), the voltage level dropped from 1.8V to 0.5V significantly. From the findings, it can be said that the selected load resistance values is unsuitable if the main objective is to have a maximum output voltage level. Having said that, the IDA-MPPT technique has an advantage of being able to stabilize the boosted voltage of the first MPPC board and stabilize the supercapacitor voltage which adequate to feed for the sec-



ond MPPC board. As a result, the MPPC has achieved a maximum of 5V level that significantly reflects the new MPPT scheme on the load behaviour of the TEM modules. At this time the current level is recorded to be at 5mA. The above results, is may due to the capability of IDA-MPPT to shape the harvested energy out of the TEM modules to meet the maximum voltage level that set by the MPPC board. From this observation, it can be said that the output load resistance plays an important role of determining the desired stabilize output level, eventhough the IDA-MPPT has boosted to the maximum rating capped by the MPPC board.

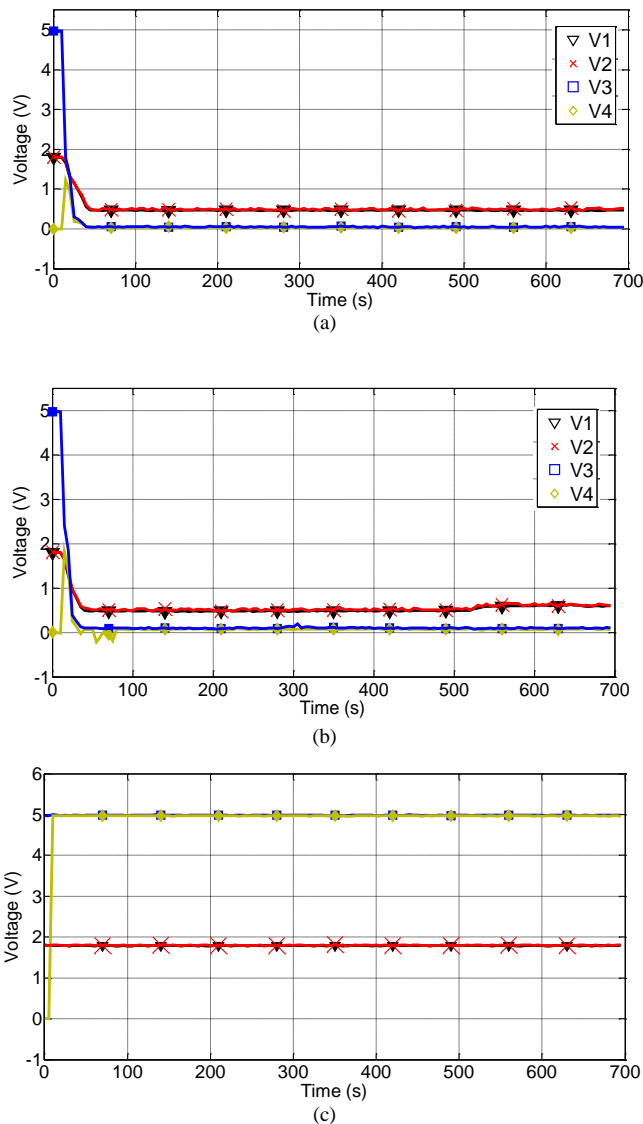


**Fig. 6:** Load dependence behavior of the TEM with IDA-MPPT. (a)  $R_L = 6.6 \Omega$ . (b)  $R_L = 13.2 \Omega$ . (c)  $R_L = 1 \text{ k}\Omega$ .

To validate further, another output loaded resistance is loaded to the system. The TEM is now loaded with a smaller load resistance of  $0.2\Omega$ , the results as shown in Fig. 7. Unlike  $R_L = 1 \text{ k}\Omega$ , with  $R_L = 0.2 \Omega$  a constant supply at a maximum voltage level for about 20s is successfully delivered. In addition, eventhough the load resistance value is smaller than the other two previous values the TEM is still able to generate with the desired response for 20s with stable output voltage level.

The level of voltage drops after 20s to a nearly zero level. This happened when the voltage level of the boosted energy of the second MPPC board decreases at the same time. In contrast, the other to load resistance values ( $R_L = 6.6\Omega$  and  $R_L = 13.2\Omega$ ), are hardly to maintain its stable voltage for certain period. The value kept changing increases and decreases through active the zones (Fig. 5 c). However, the only disadvantage, of the  $R_L = 0.2\Omega$ , is the measured current to have at 25A, which very high for certain device applications.

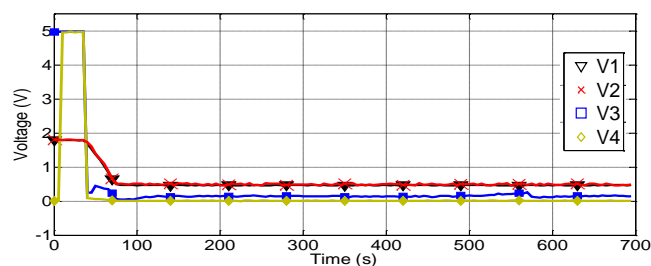


**Fig. 7:** Load dependence behavior of the TEM with IDA-MPPT and  $R_L = 0.2 \Omega$ .

The next important experiment would be an empirical analysis that would determine the range of loaded resistance value that capable to generate its maximum value as capped by the specified MPPT board. In this subsection, several load resistor values were used and analyse that can maintain the system performance in term of its stability and allow the TEM to achieve it maximum operating point. The specified voltage notations of all the points as shown in Fig. 3 (IDA-MPPT technique) is also labelled and plotted on Fig. 8.

The selected load resistance values starts from as small as  $10\Omega$  and up to the possible maximum value of  $200k\Omega$ . Fig. 8 shows that the 5V voltage output can be obtained starting from resistor value of  $200\Omega$ , then proceed to higher values. Load resistance less then this value, is incapable of achieving 5V voltage level. From this observation, it indicates that the system can be maintained and stabilize when the loaded resistance value starts from  $200\Omega$  and would retain the same effect until  $200k\Omega$ . This analysis is referring to the specified voltage test points of  $V_1$  and  $V_2$ . When the voltage at the test points  $V_1$  and  $V_2$  reaches a value of approximately 1.7V, the arrangement of the modular system can increase the output voltage load resistance up to the level of 5V. Therefore, when the first MPPT board reaches 1.7 V, the output energy of first MPPT board can be fed to the second MPPT board in order for the load resistance value to reach its maximum level.

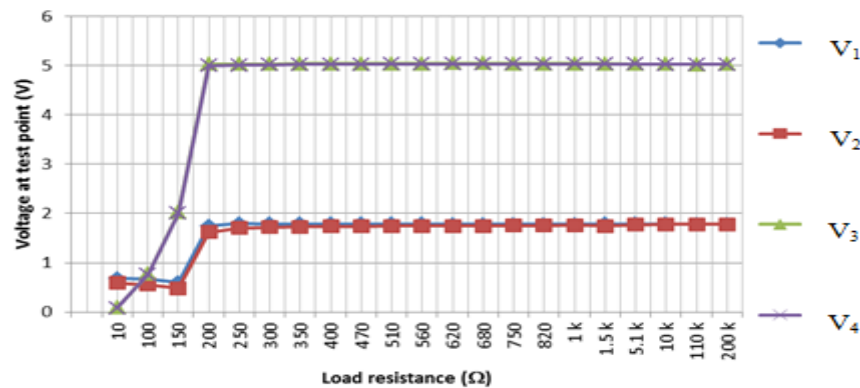


Fig. 8: Rated voltage at the test point for different values of the load resistor.

The results analysis have shown the load dependance behaviour of the system with the proposed IDA-MPPT technique, in which it has several merits.

- i. The control strategy adopted, can significantly transfer energy one device to another device, where the level of energy is closely dependent with the load resistance values. This observation has attributed to the behaviour of the predetermined voltages at several test points. As a result it shows that with the implementation IDA-MPPT technique, the load can still receive minimal energy regardless of the load resistance values,.
- ii. When changing the load resistance value to  $1k\Omega$ , a response was recorded at all voltage test points. It was found out the 5V voltage level can be maintain throughout the analysis. The results from the first MPPT board that was capped at 1.8V can certainly boost the voltage level of the second MPPT to its maximum rating. Even the recorded current by the load resistor is so small compared to the others. Typical values of the currents is smaller than 25 mA based on the results shown in Fig. 6.
- iii. With the combination of the proposed technique with common MPPT, the load behaviour analysis significantly determine the best load resistance values that can achieved maximum at the load side. The end load voltage can surely portray the behaviour in exponential equivalent form of the IDA for the correct voltage level.
- iv. The overall performance of the IDA-MPPT technique, has shown that 83.33% efficiency is generated when loaded with  $1k\Omega$  resistor, which significantly higher with the system without IDA-MPPT (30%). An increment of more than 60% difference shows that energy is being delivered at high efficiency when the high resistance values were loaded.

## 4. Conclusion

This paper has presented a technique to harvest energy from TEM modules incorporated with load dependence behavior using proposed IDA-MPPT technique. From the simulation and the experimental results have shown that the IDA-MPPT technique is significantly robust in order to enhance the energy delivery stability. It has been proven and found that the behavior of the load at the end is significantly influent by the new proposed TEM model scheme. The predetermined test voltage will behave differently which depending on the value of the load resistance values. This is proven with the active zone analysis where the system can supply energy to a different level, and is significantly influenced by the loaded impedance at the end. The modules started with the energy harvester of TEM modules, and employed of existing MPPT scheme with different load impedances, thus from the verification it has shown that MPPT schemes are required to maintain the load voltage at a 5V stable voltage line. Then it is followed by the employment of the IDA-MPPT technique that significantly controls its input energy to shape similarly to the output response. To provide additional evidence of the effect, further analysis was carried using lower load resistance values. It has been shown that  $R_L = 1k\Omega$  was found out to be the best load resistance value for the proposed scheme. In this study, the new proposed MPPT circuit on the overall TEM behavior is extensively discussed in terms of its output voltage and current characteristics, stability and loading effect. This will help future researchers to choose a suitable load impedance to be connected to the TEM to ensure the TEM operates within its maximum capability.

## Acknowledgement

The authors would like to thank the Department of Industrial Electronic, Faculty of Electronic and Computer Engineering, University Technical Malaysia Melaka (UTeM) with Grant No. FRGS/1/2017/TK07/FKEKK-CETRI/F0033, Department of Electrical, Electronic,

and Systems Engineering, Faculty of Engineering and Built Environment, Universiti Kebangsaan Malaysia (UKM) under Project Code GGP-2017-011, and the Ministry of Higher Education for the operational and financial support for this project.

## References

- [1] Batal MA, Nashed G & Jneed FH, "Conductivity and thermoelectric properties of nanostructure tin oxide thin films", *Journal of the Association of Arab Universities for Basic and Applied Sciences*, Vol. 15, (2014), pp. 15-20.
- [2] Dai D, Zhou Y & Liu J, "Liquid metal based thermoelectric generation system for waste heat recovery". *Renewable Energy*, Vol. 36, No. 12, (2011), pp. 3530-3536.
- [3] Lesage FJ & Pagé-Potvin N, "Experimental analysis of peak power output of a thermoelectric liquid-to-liquid generator under an increasing electrical load resistance", *Energy Conversion and Management* Vol. 66, (2013), pp. 98-105.
- [4] Lesage FJ, Sempels ÉV & Lalonde-Bertrand N, "A study on heat transfer enhancement using flow channel inserts for thermoelectric power generation", *Energy Conversion and Management*, Vol. 75, (2013), pp. 532-541.
- [5] Rabari R, Mahmud S & Dutta A, "Numerical simulation of nanostructured thermoelectric generator considering surface to surrounding convection", *International Communications in Heat and Mass Transfer*, Vol. 56, (2014), pp. 146-151.
- [6] Yu X, Xu D, Liu Y, Zhou H, Wang Y, Gao X, Feng F, Wang Y & Li T, "Significant performance improvement for micro-thermoelectric energy generator based on system analysis", *International Journal of Electrical Power & Energy Systems*, Vol. 67, (2015), pp. 417-422.
- [7] Admasu BT, Luo X & Yao J, "Effects of temperature non-uniformity over the heat spreader on the outputs of thermoelectric power generation system", *Energy Conversion and Management*, Vol. 76, (2013), pp. 533-540.
- [8] Yusop AM, Mohamed R & Ayob A, "Model building of thermoelectric generator exposed to dynamic transient sources" *IOP Conference Series: Materials Science and Engineering*, Vol. 53, Conf. 1, (2013), pp. 1-9, doi:10.1088/1757-899X/53/1/012015.
- [9] Ma M & Yu J, "An analysis on a two-stage cascade thermoelectric cooler for electronics cooling applications", *International Journal of Refrigeration*, Vol. 38, (2014), pp. 352-357.
- [10] Chen W.-H, Liao C.-Y & Hung C.-I, "A numerical study on the performance of miniature thermoelectric cooler affected by Thomson effect", *Applied Energy*, Vol. 89, No. 1, (2012), pp. 464-473.
- [11] Meng J.-H, Wang X.-D & Zhang X.-X, "Transient modeling and dynamic characteristics of thermoelectric cooler", *Applied Energy*, Vol. 108, (2013), pp. 340-48.
- [12] Nuwayhid RY, Rowe DM & Min G. "Low cost stove-top thermoelectric generator for regions with unreliable electricity supply", *Renewable Energy*, Vol. 28, No 2, (2003), pp. 205-222.
- [13] Nuwayhid RY, Shihadeh A & Ghaddar N, "Development and testing of a domestic woodstove thermoelectric generator with natural convection cooling", *Energy Conversion and Management*, Vol. 46, No. 9-10, (2005), pp. 1631-1643.
- [14] O'shaughnessy SM, Deasy MJ, Kinsella CE, Doyle JV & Robinson AJ, "Small scale electricity generation from a portable biomass cookstove: Prototype design and preliminary results", *Applied Energy*, Vol 102, (2013), pp. 374-385
- [15] Xu Y, Yuan Y & Fu J, "Modeling and design for a thermoelectric charger", *2012 IEEE International Symposium on Industrial Electronics (ISIE)*, (2012), pp. 383-386, doi: 10.1109/ISIE.2012.6237116.
- [16] Zhao W, Choi K, Bauman S, Salter T, Lowy DA, Peckerar M & Khandani MK, "An energy harvesting system surveyed for a variety of unattended electronic applications". *Solid-State Electronics*, Vol. 79, (2013), pp. 233-237.
- [17] Liu, X., Li C, Deng YD & Su CQ, "An energy-harvesting system using thermoelectric power generation for automotive application. *International Journal of Electrical Power & Energy Systems*, Vol. 67, (2015), pp. 510-516.
- [18] Liang X, Sun X, Tian H, Shu G, Wang Y & Wang X, "Comparison and parameter optimization of a two-stage thermoelectric generator using high temperature exhaust of internal combustion engine", *Applied Energy*, Vol. 130, (2014), pp. 190-199.
- [19] Stevens RJ, Weinstein SJ & Koppula KS, "Theoretical limits of thermoelectric power generation from exhaust gases", *Applied Energy*, Vol. 133, (2014), pp. 80-88.
- [20] He W, Zhou J, Hou J, Chen C & Ji J, "Theoretical and experimental investigation on a thermoelectric cooling and heating system driven by solar", *Applied Energy*, Vol. 107, (2013), pp. 89-97.
- [21] Jieting W, Linchang X & Hao W, "The study of thermoelectric power generation in the cooling of fin and vibration heat pipe". *Energy Procedia*, Vol. 17, Part B, (2012), pp. 1570-1577.
- [22] Riffat SB, Omer SA & Ma X. "A novel thermoelectric refrigeration system employing heat pipes and a phase change material: An experimental investigation", *Renewable Energy*, Vol. 23, No 2, (2001), pp. 313-323.
- [23] Marek Z & Hartmut B, "Modelling of seebeck effect in electron beam deep welding of dissimilar metals", *COMPEL - The international journal for computation and mathematics in electrical and electronic engineering*, Vol. 28, No 1, (2009), pp. 140-153.
- [24] Carmo JP, Antunes J, Silva MF, Ribeiro JF, Goncalves LM & Correia JH, "Characterization of thermoelectric generators by measuring the load-dependence behavior". *Measurement*, Vol. 44, No. 10, (2011), pp. 2194-2199.
- [25] Karabetoglu S, Sisman A, Ozturk ZF & Sahin T, "Characterization of a thermoelectric generator at low temperatures", *Energy Conversion and Management*, Vol.62, (2012), pp. 47-50.
- [26] Kossyvakis DN, Vossou CG, Provatidis CG & Hristoforou EV, "Computational and experimental analysis of a commercially available seebeck module", *Renewable Energy*, Vol. 74, (2015), pp. 1-10.
- [27] Yusop AM, Mohamed R & Mohamed A, "Inverse dynamic analysis type of mppt control strategy in a thermoelectric-solar hybrid energy harvesting system", *Renewable Energy*, Vol. 86, (2016), pp. 682-692.
- [28] Mohamed R, Yusop AM, Mohamed A & Nordin NI, "Behavioral analysis of thermoelectric module under different configurations and temperature gradient", *Jurnal Kejuruteraan*, Vol. 28, (2016), pp. 19-27.
- [29] Yusop AM, Mohamed R, Ayob A & Mohamed A, "Dynamic modeling and simulation of a thermoelectric-solar hybrid energy system using an inverse dynamic analysis input shaper", *Modelling and Simulation in Engineering*, Vol. 2014, Article ID 376781, (2014), pp. 1-22.
- [30] Yusop AM, Mohamed R & Ayob A, "Model building and behavior analysis of thermoelectric-solar hybrid energy system exposed to dynamic sources", *2013 IEEE Student Conference on Research and Development*, Article No. 7002627, (2013), pp. 439-443, doi: 10.1109/SCORED.2013.7002627